CHALMERS

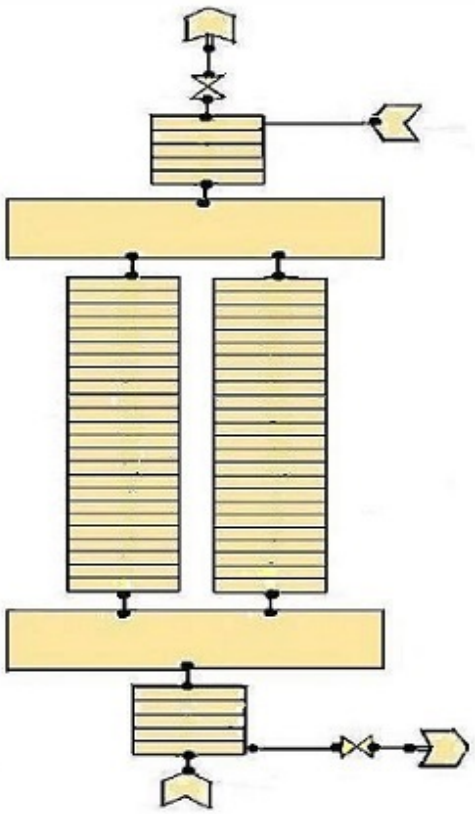

On the development of a TRACE model for the study of reflooding in BWR parallel channels

Master's Thesis

Md.Ghulam Zakir

Department of Applied Physics
Division of Nuclear Engineering
CHALMERS UNIVERSITY OF TECHNOLOGY
Gothenburg, Sweden 2015

CTH-NT-305

On the development of a TRACE model for the study of reflooding in BWR parallel channels

Md.Ghulam Zakir

Department of Applied Physics

Division of nuclear engineering

CHALMERS UNIVERSITY OF TECHNOLOGY

Gothenburg, Sweden 2015

On the development of a TRACE model for the study of reflooding in a BWR parallel channels.

Md.Ghulam Zakir

Master's Thesis

CTH-NT-305

ISSN 1653-4662

Department of Applied Physics

Division of Nuclear Engineering

Chalmers University of Technology

SE-41296, Gothenburg.

Sweden.

Gothenburg, Sweden 2015

On the development of TRACE model for study of reflooding in BWR parallel channel

Md.Ghulam Zakir

Division of Nuclear Engineering

Department of Applied Physics

Chalmers University of Technology

Abstract

In a Loss-Of-Coolant accident in a Boiling Water Reactor, heat generated in the nuclear fuel is not properly removed because of the deterioration of the coolant mass flow rate in the reactor core. This fact leads to an increase of the fuel temperature that can cause damage to the core and leakage of the radioactive fission products. In order to reflood the core and stop the increase of temperature, an emergency core cooling system delivers water under this kind of conditions.

The current work is an investigation of how the power distribution between two channels can affect the process of reflooding when the emergency water is injected from the top of the channels. To do so, the thermal-hydraulic system code TRACE has been used. Therefore a TRACE model of the two heated channels has been developed, and three hypothetical cases with different power distributions have been studied.

Keywords: LOCA, TRACE, ECCS, PCT.

Acknowledgements

First of all I would like to thank the almighty for giving me health and strength in my life.

My sincerest gratitude goes to my supervisor Professor Paolo Vinai, who has supported me with his extraordinary knowledge and patience throughout my thesis work. He was always there to provide enough guidance and showed me different ways to approach a research problem. His wonderful teaching made me interested in thermohydraulics part of reactor safety system and helped me start this thesis. Without his encouragement and support this research would have not been possible. Moreover, I would like to thank Dr.Manuel Calleja for his valuable comments throughout my research period.

My scholarship program has been funded by Ministry of Science and technology, Bangladesh. I want to thank Mohammad Saifullah, project director of Bangabandhu Fellowship and ICT project for giving me such an opportunity and for monitoring my regular work progress. I would also like to thank Mr. Majharul Habib for his inspiration and motivation throughout this whole period of my MSc degree.

Finally, I would like to thank my elder brother and my parents for supporting me throughout my studies and giving me the moral support to go for the higher studies.

With lots of thanks,

Md. Ghulam Zakir

Goteborg, Sweden, 2015.

Contents

List of figures

List of tables

ABBREVIATIONS

BWR	Boiling Water Reactor
CCFL	Counter Current Flow
ECCS	Emergency Core Cooling System
GHG	Green House Gases
LOCA	Loss Of Coolant Accident
LWR	Light Water Reactor
NPP	Nuclear Power Plant
NRC	Nuclear Regulatory Comission
PWR	Pressurized Water Reactor

Chapter 1

Introduction

1.1 Nuclear energy

Nuclear energy has become an important part of world electricity generation system. 16% of total world electricity demand is fulfilled by approximately four hundred and thirty nuclear reactors located in 30 different countries. In addition to this, almost half of this number of reactors will operate for several decades in the future. The energy demand in both developed and developing countries will be doubled by the end of 2030 and electricity consumption will increase by 50%. The situation will be critical in developing countries where energy crisis results in economic problems, poverty as well as low life standards. Nuclear power can make a significant contribution to eliminate this energy crisis with its low running cost and energy security. In addition to this, abundance of natural uranium resource is 14.8 million tons which can provide nuclear energy for the next 270 years. Furthermore, technical advancements can enhance the efficiency of nuclear power plants and spent nuclear fuel reprocessing techniques can solve the economic problems if Uranium price goes high. So far several technologies have been implemented to convert the nuclear energy into electrical energy. However, light water reactor (LWR) technologies, pressurized water reactor (PWR) and boiling water reactor (BWR), have become well-known since these technologies are used in the majority of power plants all over the world. Nuclear power plants have comparatively lower greenhouse gas (GHG) emission which offers a great opportunity to replace the fossil fuel based energy system by nuclear power. At the same time, construction of high level waste management repositories and decreasing cost of disposal can make the technology more global and comprehensive. Several features such as safe nuclear operation, lower dose to the workers and lower probability of accident in nuclear reactor can make this technology more reliable than before. [1] [2]

1.2 How a LWR works

The majority of commercial nuclear power plants are Light Water Reactors (LWRs). In this type of reactors light water is used to remove the heat generated by the nuclear fissions in the reactor core, and to moderate the neutrons needed for fissioning the relatively low-enriched nuclear fuel.

LWRs can be mainly Pressurized Water Reactor (PWRs) and Boiling Water Reactors (BWRs). In the first case, boiling is not allowed in the reactor core and steam is generated on a secondary side by making use of steam generators. In the second case, the steam is directly produced in the reactor core. Then the high energetic steam interacts with the turbine and the turbine converts its kinetic energy into rotational energy and generates electricity, the same electricity generation procedure that can occur in a conventional gas turbine.[3] [4]

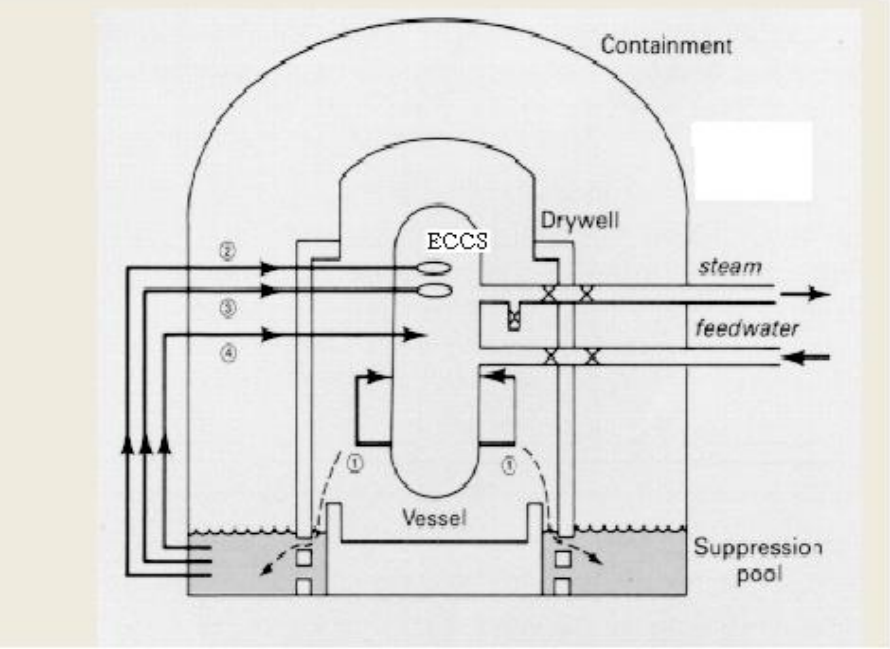

Figure 1.1:A BWR with ECCS surrounded by the containment with other equipment [5].

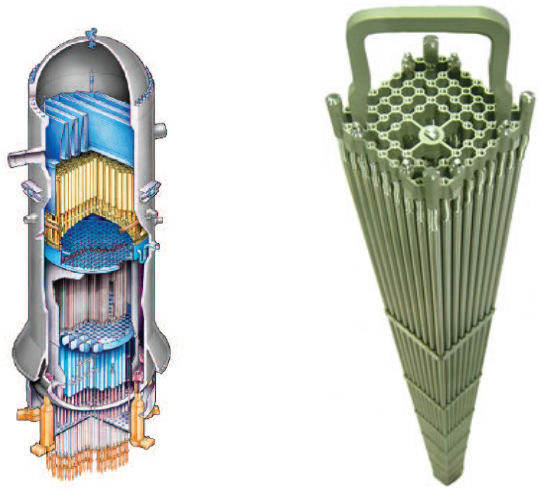

(a) (b)

Figure 1.2 : Core inside a BWR (a) and fuel assembly (b) [6].

1.3 Nuclear Reactor Safety

Safety is one of the fundamental requirements for development and expansion of nuclear industry. In fact a nuclear power plant (NPP) contains a large inventory of radioactive materials which are considered as potential health hazard for public and environment. The Safety of nuclear power plants (NPPs) is not only related to safe nuclear operation but also associated with minimizing the consequence of severe nuclear accidents. Nuclear reactor safety is based on the concept of defense-in-depth. The objective of defense-in-depth is to compensate for the human and component failures, to maintain effectiveness of the physical barriers, to protect the public and environment from harm. Accordingly, several physical barriers for the radioactive fission products are implemented together with different levels of protection. The levels of protection are mainly based on a careful design of the plant that includes several safety features.

One of the crucial aspects in nuclear power plant safety involves the analysis of large break loss-of-coolant accidents (LOCAs). In this kind of scenario, the inventory of core coolant is lost from a break in one of the main pipes. Thus the heat generated because of the decay of the fission products in the core cannot be removed and the temperature of the fuel rods increases. In order to avoid severe damage of the core, an emergency core cooling system is used to provide water in the case of a LOCA. The water delivered by this safety system can stop the temperature increase in the core, and prevent the core from melting.

In BWRs the emergency water can be injected from the top of the core, so that the core can be reflooded and the cooling of the fuel rods can occur.

1.4 Objective and structure of the thesis

1.4.1 Objective

This thesis investigates the reflooding phase in two parallel heated channels in a BWR during large break loss of coolant accident (LOCA).

The current work is an investigation of how the power distribution between two channels can affect the process of reflooding when the emergency water is injected from the top of the channels. To do so, the thermal-hydraulic system code TRACE has been used. Therefore a TRACE model of the two heated channels has been developed, and three hypothetical cases with different power distributions have been studied.

1.4.2 Methodology

The entire thesis work can be summarized as follows:

- Literature study: Understanding of TRACE code by its two volumes of manuals and study of the research article related to the experiment.
- Preparation of the model and a closer look at it: Preparation of one dimensional model by TRACE code and variation in inlet boundary condition to obtain the correct result.

1.4.3 Structure of the report

Chapter 1 contains the *Introduction* of the report. *Descriptions of different tools* are discussed in chapter 2. Chapter 3 gives the entire *Description of the model.* The *simulations and analysis of the result* of the simulation is described in the chapter 4. Finally, *summary and conclusion* are mentioned in Chapter 5.

Chapter 2

Description of the tools

In this study, two different tools are used to execute the entire task: TRACE and Aptplot. The construction of the model and the thermal-hydraulic simulation process are carried out with TRACE and the plots are prepared with Aptplot. In this chapter, the two tools are described.

2.1 TRACE

TRACE is a thermal-hydraulic system code that was developed with the support of the U.S. Nuclear Regulation Commission (NRC). This code is used for safety analysis of LWRs. In particular, it can be applied to study operational and accidental transients, as, for instance, LOCAs in a BWR.

The code is based on the numerical solution of the conservation equations for two-phase flow. In this context, the equations of mass, momentum and energy for the vapor and liquid phases are:

2.1.1 Time Averaged Mass Equations

$$\frac{\partial[(1-\alpha)\bar{\rho}_l]}{\partial t} + \nabla.\left[(1-\alpha)\bar{\rho}_l\vec{\bar{v}}_l\right] = -\Gamma \qquad (2.1)$$

$$\frac{\partial(\alpha\bar{\rho}_g)}{\partial t} + \nabla.\left[\alpha\bar{\rho}_g\vec{\bar{v}}_g\right] = \Gamma \qquad (2.2)$$

In equations (2.1) and (2.2) over bar defines time average, α represents gas volume fraction. Time averaged interface jump condition to transfer mass is denoted by Γ .The term “g” and “l” represents gas specific and liquid specific terms.

2.1.2 Time Averaged Energy Equations:

$$\frac{\partial\left[(1-\alpha)\bar{\rho}_l\overline{\left(e_l+\frac{v_l^2}{2}\right)}\right]}{\partial t} + \nabla.\left[(1-\alpha)\bar{\rho}_l\,\overline{\left(e_l+\frac{v_l^2}{2}\right)\vec{v}_l}\right]$$

$$= -\nabla\left[(1-\alpha)\vec{\bar{q}}_l'\right] + \nabla.\left[(1-\alpha)\left(\overline{T_l.\vec{V}_l}\right)\right] + (1-\alpha)\bar{\rho}_l\overline{g.\vec{V}_l} - \bar{E}_i + \overline{q_{dl}} \quad (2.3)$$

$$\frac{\partial\left[\alpha\bar{\rho}_g\overline{\left(e_g+\frac{v_g^2}{2}\right)}\right]}{\partial t} + \nabla.\left[\alpha\bar{\rho}_g\overline{\left(e_g+\frac{v_g^2}{2}\right)\vec{v}_g}\right]$$

$$= -\nabla\left[\alpha\vec{\bar{q}}_g'\right] + \nabla.\left[\alpha\left(\overline{T_g.\vec{V}_g}\right)\right] + \alpha\bar{\rho}_g\overline{g.\vec{V}_l} + \bar{E}_i + \overline{q_{dg}} \quad (2.4)$$

In the above two equations (2.3) and (2.4), $\bar{E}$ represents time averaged interface jump condition to transfer energy. In addition to this, q is conductive heat flux and q_d is direct heat or radioactive decay heat, and T is full stress tensor.

2.1.3 Time Averaged Momentum Equations:

$$\frac{\partial[(1-\alpha)\bar{\rho}_l\vec{\bar{v}}_l]}{\partial t} + \nabla.\left[(1-\alpha)\bar{\rho}_l\overline{\vec{v}_l\vec{v}_l}\right] = \nabla[(1-\alpha)\bar{T}_l] + (1-\alpha)\bar{\rho}_l\vec{g} - \bar{M}_i \quad (2.5)$$

$$\frac{\partial[\alpha\bar{\rho}_g\vec{\bar{v}}_g]}{\partial t} + \nabla.\alpha\bar{\rho}_g\overline{\vec{v}_g\vec{v}_g} = \nabla\left[\alpha\bar{T}_g\right] + \alpha\bar{\rho}_g\vec{g} + \bar{M}_i \quad (2.6)$$

In the above two equations, $\bar{M}_i$represents time averaged interface jump condition to transfer momentum.

2.1.4 Volume Averaged Mass Equations:

$$\frac{\partial\overline{[(1-\alpha)\rho_l]}}{\partial t} + \overline{\nabla.\left[(1-\alpha)\rho_l\vec{\bar{v}}_l\right]} = -\bar{\Gamma} \quad (2.7)$$

$$\frac{\partial(\overline{\alpha\rho_g})}{\partial t} + \nabla.\left[\overline{\alpha\rho_g\vec{\bar{v}}_g}\right] = \bar{\Gamma} \quad (2.8)$$

2.1.5Volume Averaged Energy Equations:

$$\frac{\partial\left[\overline{(1-\alpha)\rho_l\left(e_l+\frac{v_l^2}{2}\right)}\right]}{\partial t} + \overline{\nabla.\left[(1-\alpha)\rho_l\left(e_l+\frac{v_l^2}{2}+\frac{P}{\rho_l}\right)\vec{\bar{v}}_l\right]}$$

$$= \overline{-\nabla\left[(1-\alpha)\vec{\bar{q}}_l'\right]} + \nabla.\left[(1-\alpha)\left(\overline{T_l.\vec{V}_l}\right)\right] + \overline{(1-\alpha)\rho_l g.\vec{V}_l - \Gamma h_l' + W_l} + \overline{q_{dl}} \quad (2.9)$$

$$\frac{\partial\left[\overline{\alpha\rho_g\left(e_g+\frac{v_g^2}{2}\right)}\right]}{\partial t} + \overline{\nabla.\left[\alpha\rho_g\left(e_g+\frac{v_g^2}{2}+\frac{P}{\rho_g}\right)\vec{\bar{v}}_g\right]}$$

$$= \overline{-\nabla\left[\alpha\vec{q}_g'\right]} + \overline{\alpha\rho_g g.\vec{V}_g} + \overline{\Gamma h_v' + W_g} + \overline{q_{dg}} \quad (2.10)$$

2.1.6Volume Averaged Momentum Equations:

$$\frac{\partial\overline{\left[(1-\alpha)\rho_l\vec{v}_l\right]}}{\partial t} + \overline{\nabla.\left[(1-\alpha)\rho_l\vec{v}_l\vec{v}_l\right]} = \overline{\nabla[(1-\alpha)R_l]} + \overline{(1-\alpha)\rho_l\vec{g} - M_l} \quad (2.11)$$

$$\frac{\partial\overline{\left[\alpha\rho_g\vec{v}_g\right]}}{\partial t} + \overline{\nabla.\left[\alpha\rho_g\vec{v}_g\vec{v}_g\right]} = \overline{\nabla\left[\alpha R_g\right]} + \overline{\alpha\rho_g\vec{g}} + \bar{M}_i \quad (2.12)$$

Physical correlations are also implemented so that the interaction between vapor and liquid phases, and heat transfer at the wall can be taken in account [7]. In addition, special models are also included in order to describe specific phenomena like, for instance, the critical heat flux or the counter-current flow limitation.

As regards the description of the physical system that is analyzed, TRACE offers the possibility to model the different components that could be part of the nuclear power plant. Here is only reported the components that are used in the current work.

FILL component: this consists of a computational volume that can be used to describe a flow boundary condition.

BREAK component: this consists of a computational volume that can be used to describe a pressure boundary condition.

PIPE component: it is used to model the hydraulic flow in a channel, duct, or pipe.

VALVE component: it is a computational model for simulating the behavior of a real valve.

PLENUM component: it is used to connect more than two pipes.

HEAT STRUCTURE component: it is used to model the heat generated from a heat source (e.g. a heated rod in a reactor core).

POWER component: it is associated to a heat structure and provides the power distribution within a heat source.[8]

2.2 Aptplot

Aptplot is a software replacing ACGrace which is developed by US nuclear regulatory commission (NRC) to associate with several other analytical codes. ACGrace is built to execute analytical result using the necessary information from NRC data bank files. This software is successfully used for plotting and data analysis; however, it is supported by UNIX operating systems instead of the Windows operating system. Therefore, Aptplot software is similar to ACGrace and this software is developed for the users working with Microsoft Windows operating system .In addition to this, Aptplot is built with the Java programming language which offers some additional features such as plug-in interface. However, this software is built by Java version 1.6, it will not be supported by versions lower than 1.5.[9]

Chapter 3

Description of the model

An input model has been developed to study the reflooding phase of LOCA conditions in a BWR. The input model consists of necessary information of the thermal hydraulic components to obtain a certain condition in a BWR. Furthermore, the TRACE code offers several code options to obtain more precise and accurate result. All the components and options used in the model are discussed in this chapter.

3.1 Description of the TRACE model

In this project a hypothetical system has been considered. Such a system consists of two parallel, vertical, heated channels that resemble two simplified BWR fuel assemblies. In fact the rod bundle used in the GOTA experiments was employed with some approximations [11].

The TRACE model of the hypothetical system is such that:

- A FILL is used to deliver water under normal conditions, from the bottom.
- The FILL component is connected to a lower pipe and this pipe delivers water to the two heated channels through the lower plenum.
- The heated channels are modeled with two pipe components associated to their own heat structures and power components.
- The heated water is collected from the outlet of the heated channels into the upper plenum.
- The upper plenum is connected to the upper pipe, and this pipe is connected to a pressure boundary condition given by a break component.
- The injection of the emergency coolant from the top of the system is modeled with a fill component connected to the upper pipe, and the break component for the pressure boundary condition is connected to the lower pipe. See figure:3.2

Therefore the model consists of in total 16 components. In total four PIPE components, two FILL components, two BREAK components, two HTSTRs and two power components have been used in the model. The PIPE component placed on the top is used to maintain thermohydraulic flow among FILL, BREAK and PLENUM components and main two PIPE components are used to maintain thermal hydraulic flow between the upper PLENUM and lower PLENUM, another PIPE component on bottom is used to maintain the thermal hydraulic flow among FILL, BREAK and PLENUM components. The two heat structures (HTSTR component) maintain thermal coupling between coolant flows along the channels with two fuel assemblies. All the heat structures and PIPE components are divided into 24 cell volumes. Each fuel assembly contains in total 64 rods. Each fuel assembly is showed on figure 3.1.The materials used for building fuel assembly are given in Table 3.1.

Table 3.1: Name of the components and the materials composed of.

Name of the components	**Materials**
Fuel rod pin	Nicrome(heater), Boron Nitride and Inconel-600
Inner channel wall (assumed but no heat structure been used)	Zircaloy

Table 3.2: All initial parameters used in the model.

Parameter	**Nominal**
Initial two bundle power on steady state(KW)	300
Inlet flow rate on steady state(kg/s)	7.0
Inlet flow rate on transient state (kg/s)	0.5
Outlet Pressure boundary condition (MPa)	0.1
Inlet water temperature on steady state(℃)	90
Inlet water temperature on transient state(℃)	60
Steam venting	Top

The FILL component is connected with the PLENUM by a PIPE component since the FILL component cannot be connected with the PLENUM component directly. Two BREAK components are used in this model: one for outlet boundary condition of coolant flow in steady state condition and another one for outlet boundary condition for coolant flow on reverse direction during the transient state. The number of rods in two fuel assemblies are shown in figure 3.1.the fuel pin is composed of Inconel-600 and boron nitride.

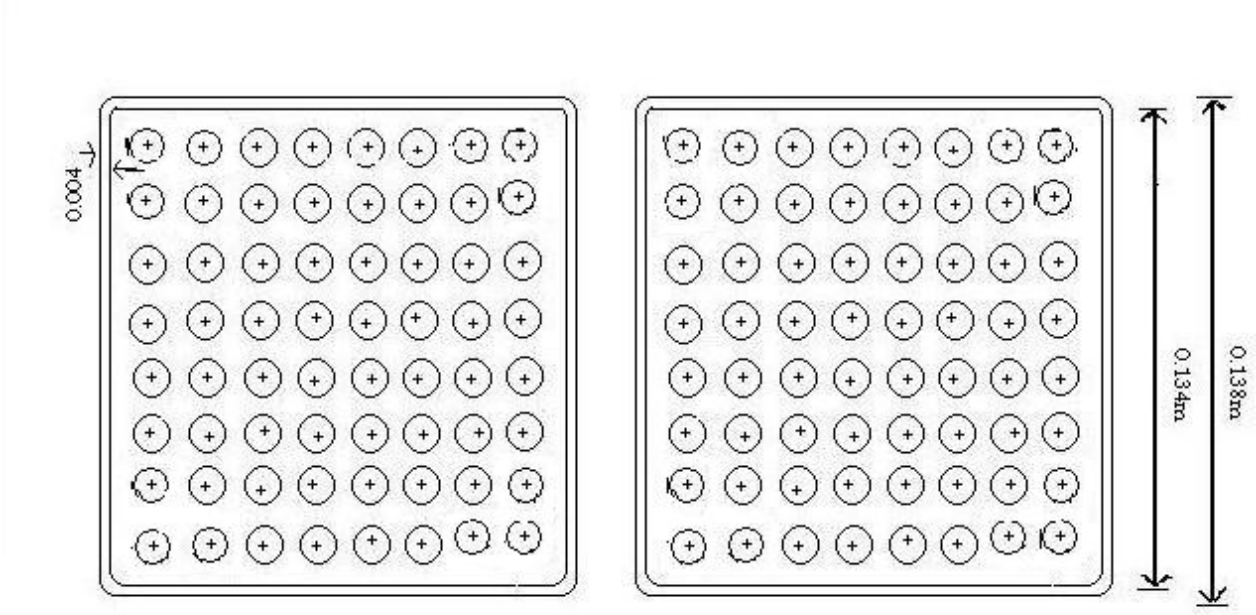

Figure 3.1: Top view of two parallel channels heated by fuel assembly.

3.2 Geometrical specification of all thermohydraulic and power components

Table 3.3: All thermohydraulic components used in this model, their id number and the parameter values.

Component ID number	Specification	No. of cells	Cell axial length[m]	Flow area[m^2]	Volume[m^3]	Hydraulic Diameter[m]
FILL, 200	For Inlet Boundary Condition	1	0.5	N/A	1.0	N/A
FILL, 100	For Inlet Boundary Condition	1	0.5	N/A	1.0	N/A
PIPE, 303	TOP CONNECTING PIPE	5	0.304	0.0208	0.0063	0.1627
PIPE,400	HEATED PIPE#1	24	0.152	0.0104	0.00158	0.0139
PIPE,500	HEATED PIPE#2	24	0.152	0.0104	0.00158	0.0139
PIPE, 300	BOTTOM CONNECTING PIPE	3	0.304	0.0208	0.0063	0.1627
BREAK,103	For outlet boundary condition on steady state condition	1	0.5	N/A	0.5	N/A
BREAK,203	For outlet boundary condition on transient condition	1	0.5	N/A	0.5	N/A
VALVE,102	Implemented on steady state condition	2	0.304	0.0208	0.0063	0.1627
VALVE,202	Implemented on	2	0.304	0.0208	0.0063	0.1627

	transient state condition					

Table 3.4: The specification thermal hydraulic single cell component PLENUM connected with several other thermal hydraulic component.

Component ID number	Specification	Number of junctions to connect other components	ID of different components it was connected with	Length of PLENUM for connecting with different components $[m]$	Volume of the PLENUM $[m^3]$
UPPER PLENUM,302	To connect FILL and BREAK components with PIPE containing Fuel Assemblies	3	PIPE,303 PIPE,400 PIPE,500	0.208 0.0104 0.0104	0.5
LOWER PLENUM,301	To connect FILL and BREAK components with PIPE containing Fuel Assemblies	3	PIPE,300 PIPE,400 PIPE,500	0.208 0.0104 0.0104	0.5

N/A: Not applicable.

Table 3.5 All the ID number HTSTR and relevant parameters.

ID number of the component	Specification	ID number of the hydraulic component that heat structure coupled with	Number of Cell	Number of elements	Number of Radial Nodes	Distance Among Different Nodes[m]
HTSTR,600	Heat structure for Heated PIPE#1	PIPE,400	24	64	3	0.0 0.005 0.006
HTSTR,700	Heat structure for Heated PIPE#2	PIPE,500	24	64	3	0.0 0.005 0.006

Table 3.5 POWER component ID number and relevant parameters.

Component ID number	Specification	ID number of the component attached with	Delivered power[KW] on steady state
POWER,601	To deliver power to Fuel Assembly 1	HTSTR600	300
POWER,701	To deliver power to Fuel Assembly 2	HTSTR700	300

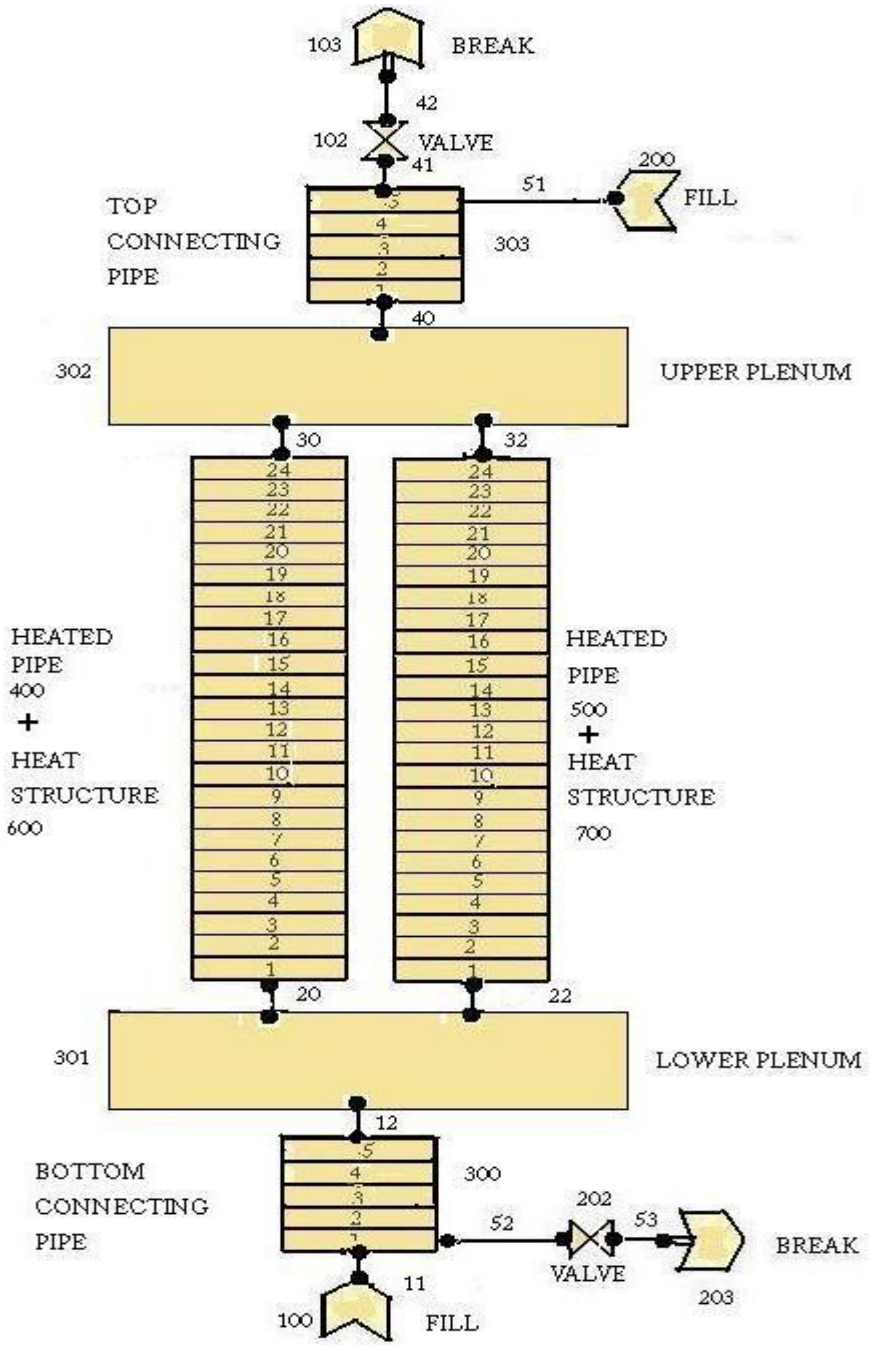

Figure 3.2: Entire thermal hydraulic model.

In the model developed two important special models for the purpose of the analysis were also selected.

For the critical heat flux, the AECL-IPPE CHF table was used, where the quality is estimated from the CISE-GE correlation. The critical heat flux is an important issue in the current context since it is related to the possible boiling crisis that a channel may suffer because of the degradation of the mass flow rate due to the loss of coolant.[10]

For the counter-current flow limitation (CCFL), the Kutateladze correlation was used [11]. If we consider the reflooding from the top of the channels, the CCFL is related to the fact that the main emergency flow that moves downwards is limited by a flow of steam moving upwards.

3.3 Simplifications used in the model

- Heated rods are all the same.
- No radial power distribution (no use of radial peaking factor).
- Axial power profile is considered uniform.

3.4 Limitations of the model

- Bypass channel is not included with the model.
- Axial conduction is not taken into account.
- Radiation from the heat structures is not been included.
- No shroud is included.
- Pressure is assumed to be constant with respect to time.

Chapter 4

Simulations and analysis of the results

The objective of this work is to perform a preliminary study of the effect of the power distribution between two heated channels on the reflooding phase of a possible LOCA. In view of this, the model illustrated in Chapter 3 was used to simulate 3 cases that differ in the power provided to the two parallel channels.

4.1 Description of the analyzed cases

Three different cases are simulated with different power levels (see the table 4.1).

Table 4.1: Initial power for the two heated channels.

Case	Initial power [kW]	
	Heated channel 1	Heated channel 2
1	300	300
2	300	295
3	300	290

In table 4.1 heated channel 1 and heated channel 2 are supplied by power component

All simulation of the 3 cases is performed in two steps. First step is defined as steady state when emergency cooling system is turned OFF and the coolant flows from the bottom to upward direction and in the second step coolant upward flow is stopped, thus, the transient state appears and emergency cooling system is turned ON to recover from the transient state. More precisely it could be explained that in the first step, spray cooling system kept OFF and the entire hypothetical test facility is operated in the steady state condition and after a while, the transient state is initiated. The spray cooling system is initiated when cladding temperature reaches the peak after 100 seconds of dry state. In the final step, coolant flow is initiated from the top and continued for 2700 seconds, however, in transient state the coolant flows in the opposite direction compared to the flow direction in steady state, meanwhile, coolant flow by FILL 100 from the bottom in steady state is kept OFF. Different states, time periods and state durations are

mentioned in table 4.2. See figure 4.1 and 4.2.Boundary conditions of FILL and BREAK components for two states of different cases are shown in figure 4.3, 4.4, 4.5, 4.6.

First, the steady state is obtained with constant boundary conditions and constant initial power.

Table 4.2 Different states, the time period and mass flow rate in different states.

State	Time period [s]	State Duration [s]	Flow Rate [Kg/s]
Steady state	0.0-200.0	200.0	7.0
Transient state	200.1-300.0	100.0	0.0
Obtaining the steady state from transient state	300.0-3000.0	2700.0	-0.5

On last column of table 4.2 the negative sign refers to the reverse direction of the flow.

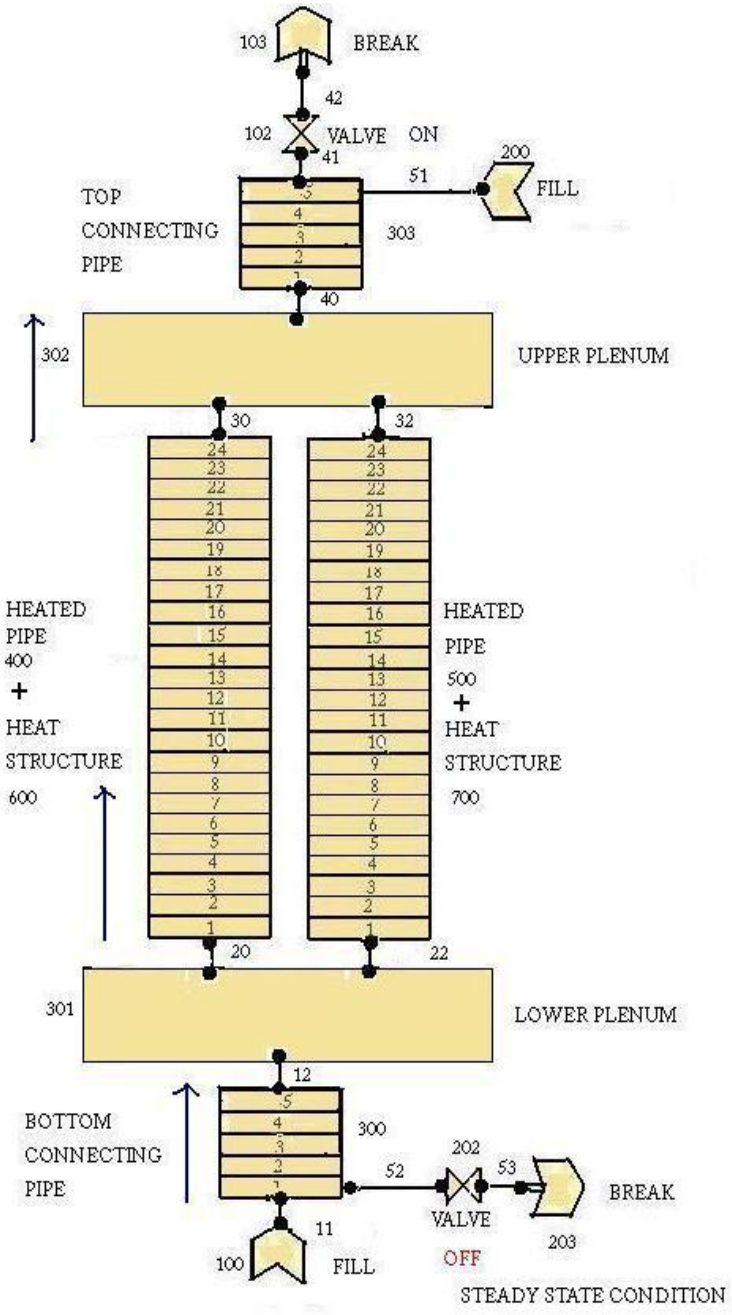

Figure 4.1: Direction of the coolant flow in steady state.

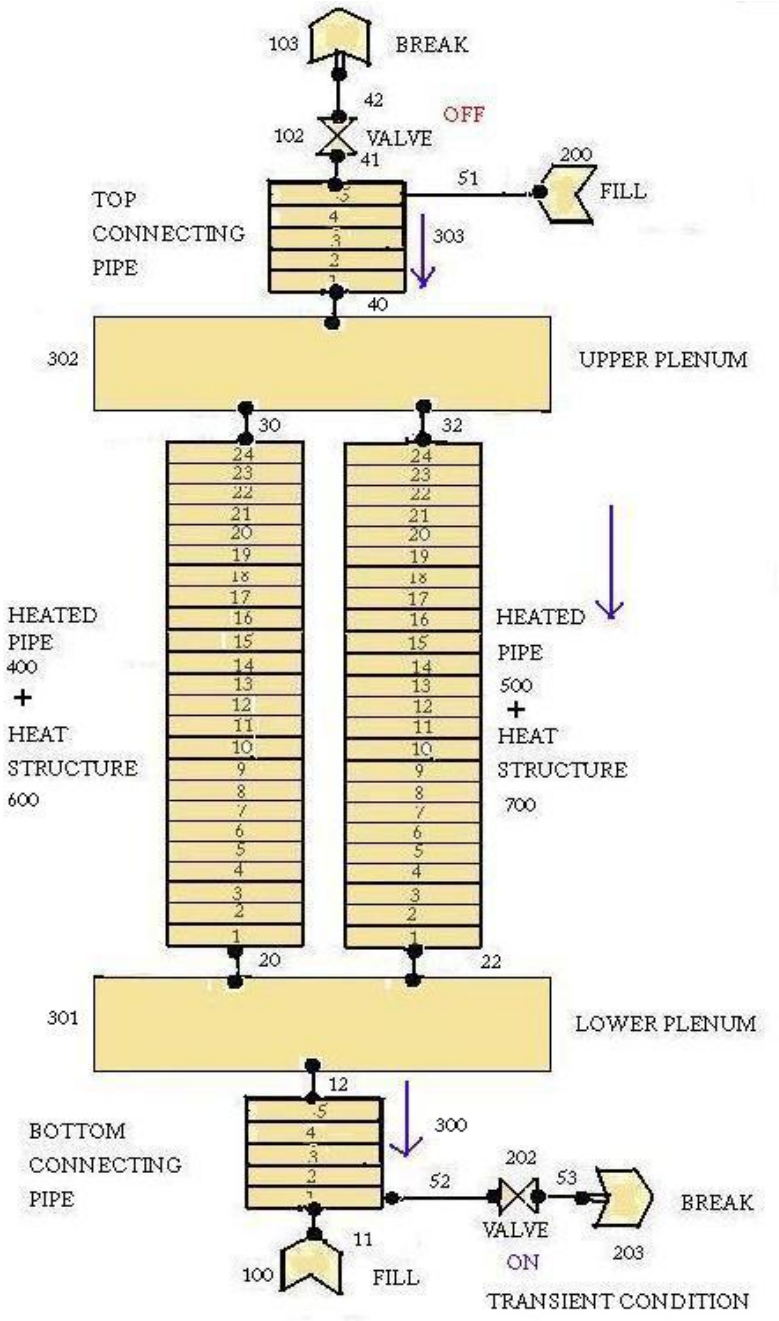

Figure 4.2: Direction of the coolant flow in transient state.

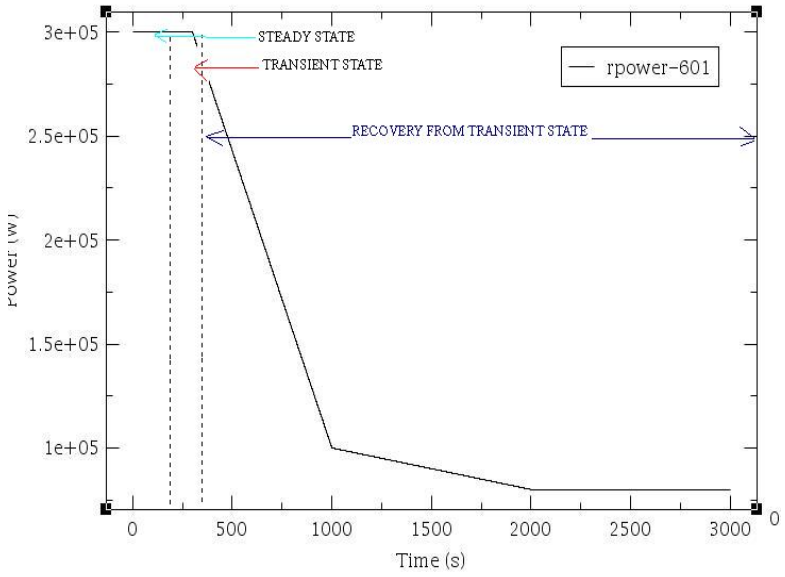

Figure 4.3: Power for fuel assemblies in different states.

In figure 4.3, the supplied power kept constant upto 300 seconds and after 300 seconds the power starts to decay exponentially .However, dry out starts after 200 seconds .Moreover, legend rpower-601 refers to the power delivered by power component 601.

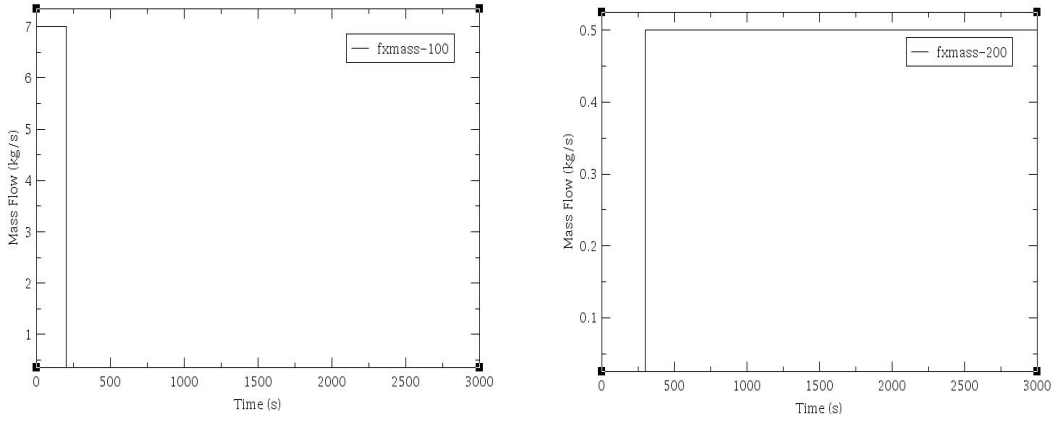

(a) **(b)**

Figure4.4:Mass flow of FILL 100 (a) and FILL 200(b).

In figure 4.4 , legend fxmass-100 and fxmass-200 refer to the mass flow rate by FILL-100 and FILL-200 component respectively.

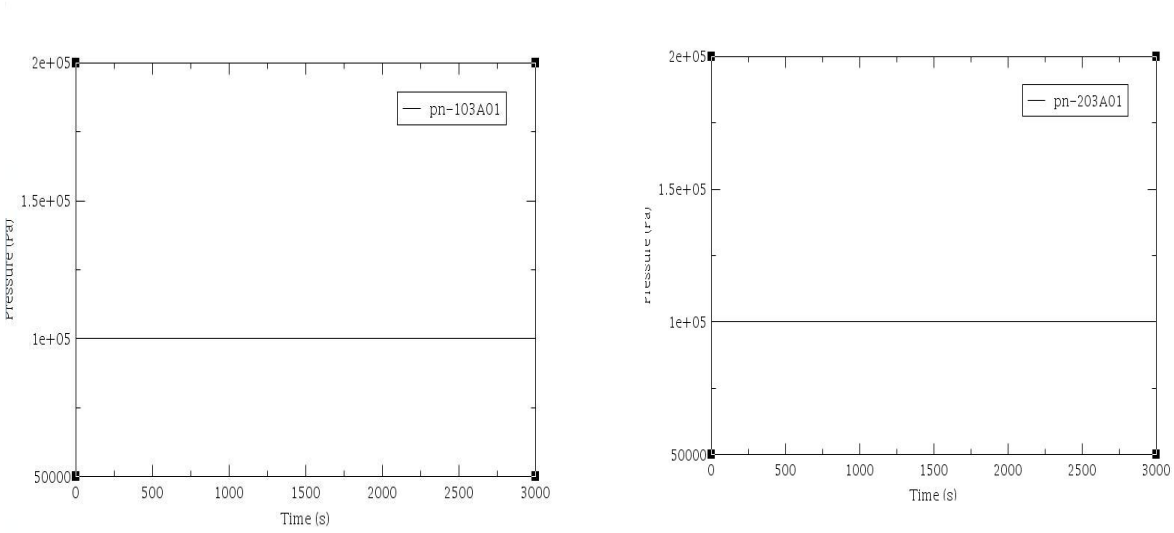

(a) **(b)**

Figure 4.5: Pressure in BREAK 103(a) and pressure in BREAK 203 (b).

In figure 4.5, legend pn-103A01 and pn-203A01 refers to the pressure in BREAK-103 and BREAK -203 component.

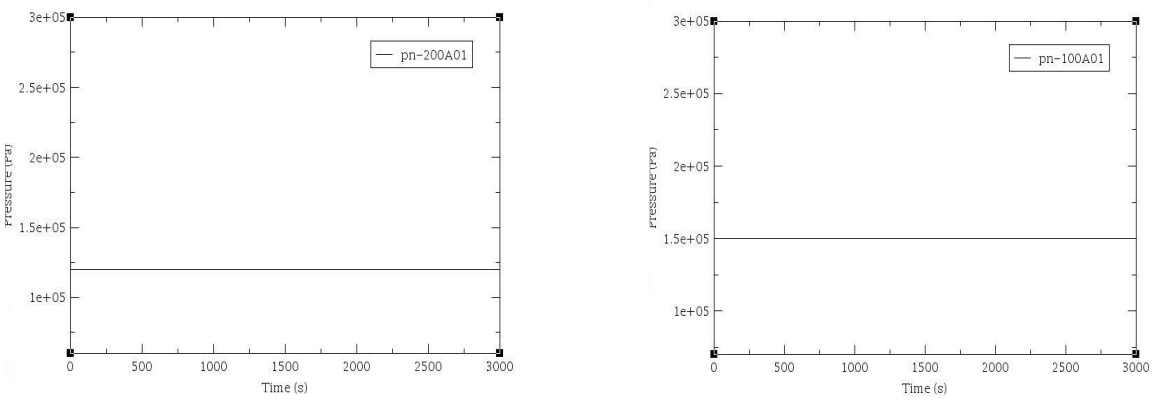

(a) **(b)**

Figure 4.6: Pressure in FILL 200(a) and pressure in BREAK 100 (b).

In figure 4.6, legend pn-200A01 and pn-100A01 refers to the pressure in FILL-200 and FILL -100 components.

4.2 Results

4.2.1 Case 1 (300-300 kW)

4.2.1.1 Steady state analysis

In steady state conditions for case 1 the mass flow rate of the two heated channel, the outer surface temperature of the fuel rod and the maximum average temperature are

identical.See:figure4.7.

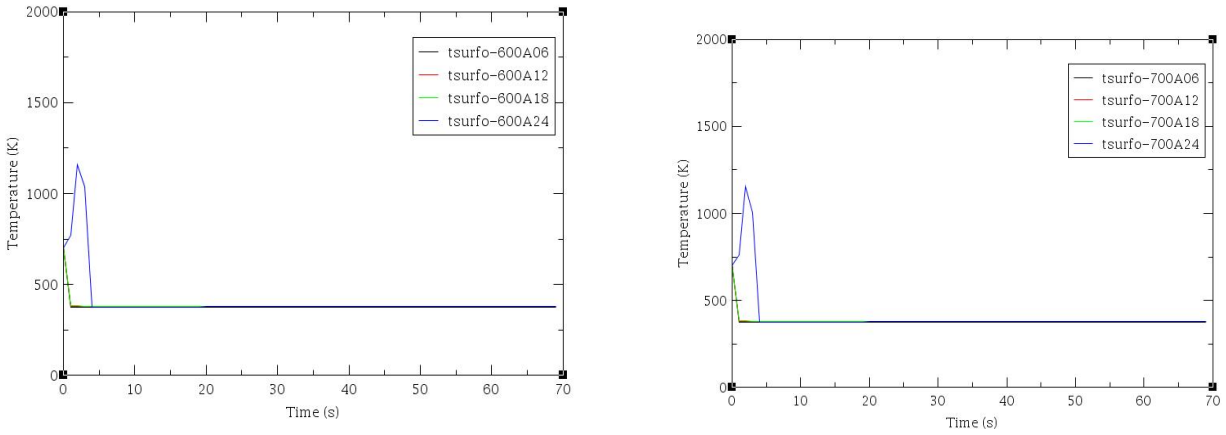

Figure4.7: Mass flow rate in two channels and fuel outer surface temperature in steady state conditions for case 1.

In figure 4.7, legend rmvm-400A12 and rmvm-500A12 refers to the mass flow rate in PIPE-400 and PIPE-500 components respectively. Moreover, legend tsurfo-600A and tsurfo-700A refers to outer surface temperature of heat structure-600 and heat structure-700 and 06,12,18 and 24 are four different level number since each PIPE is discretized in 24 different level.

4.2.1.2 Transient analysis

The upper part of the rod is cooled before the lower part of heat structure 600, at the axial levels 6, 12, 18, 24 and the temperature of the surface of the rod reaches the saturation temperature of the fluid.

The same plot is with outer surf rod temperature for heat structures 700, at the same axial levels. As expected, the two heat structures have the same behavior since the two heated channels are equal. See: figure: 4.8.

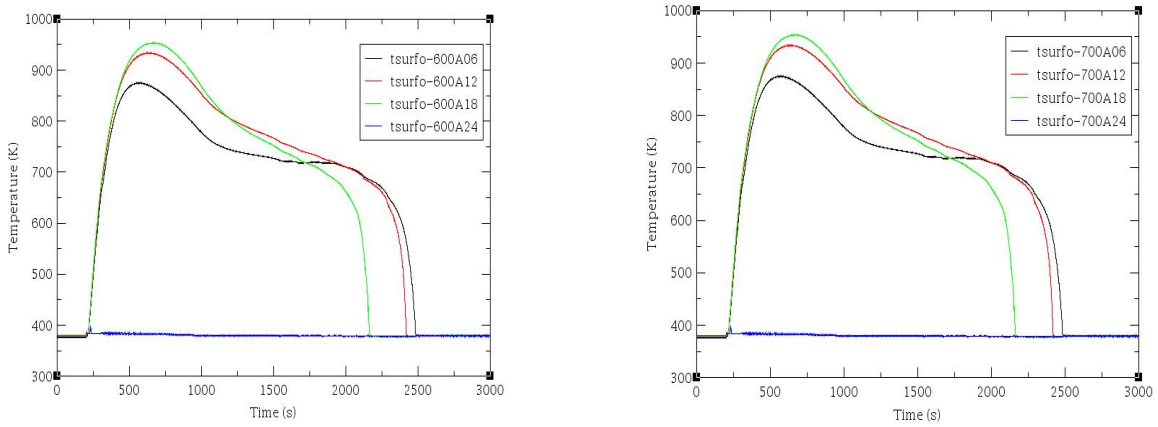

Figure 4.8: Mass flow rate in two channels and fuel outer surface temperature on transient state condition for case 1.

4.2.2 Case 2 (300-295 kW)

4.2.2.1 Steady state analysis

Delivered power on htstr 700 is a bit lower than htstr 600, however, outer surface temperatures for htstr 700 equals to the one for htstr 600. See: figure: 4.9.

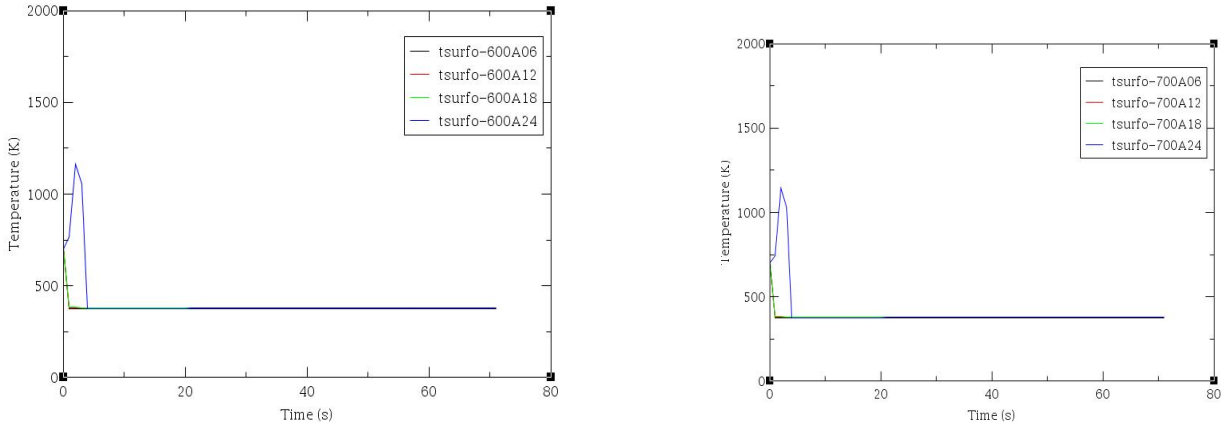

Figure 4.9: Maximum average rod temperature, mass flow rate in two channels and fuel outer surface temperature in steady state condition for case 2.

4.2.2.2 Transient analysis

Mass flow rate for pipes 400 and 500 at axial level 12 shows that in the colder channel the mass flow rate is larger (in absolute value).

The plots show the outer surface fuel temperature for heat structures 600 and for heat structure 700, at the axial levels 6, 12, 18, 24. Those plots show that the upper part of the rod is cooled

before the lower part. The outer surface temperature for htstr 700 reaches the saturation earlier than the htstr 600.See figure: 4.10.

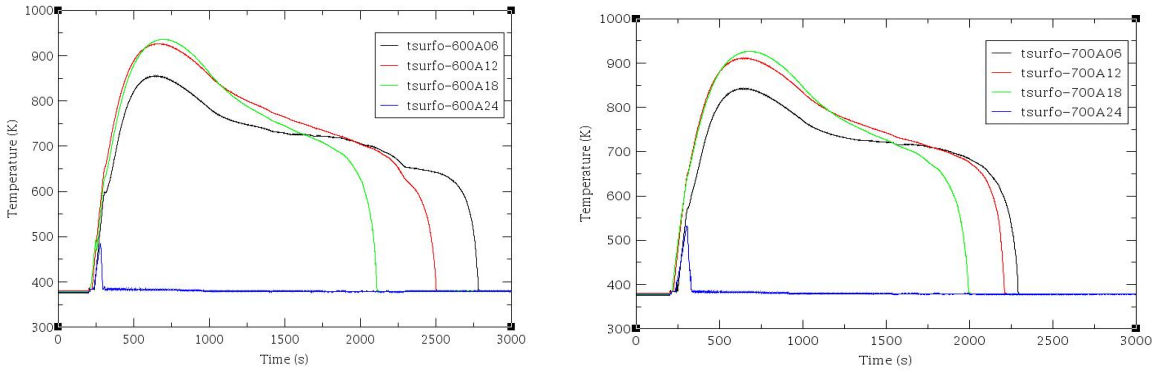

Figure 4.10: Mass flow rate in two channels and fuel outer surface temperature on transient state condition for case 2.

4.2.3 Case 3 (300-290 KW)

4.2.3.1Steady state analysis

In this case, delivered power difference between two fuel assemblies are comparatively higher than previous two cases. As a result, more discrepancy of maximum average fuel rod temperature and fuel outer surface temperature between htstr 600 and htstr 700 is evaluated. Difference between mass flow rates of two fuel assemblies are found too. See: figure:4.11

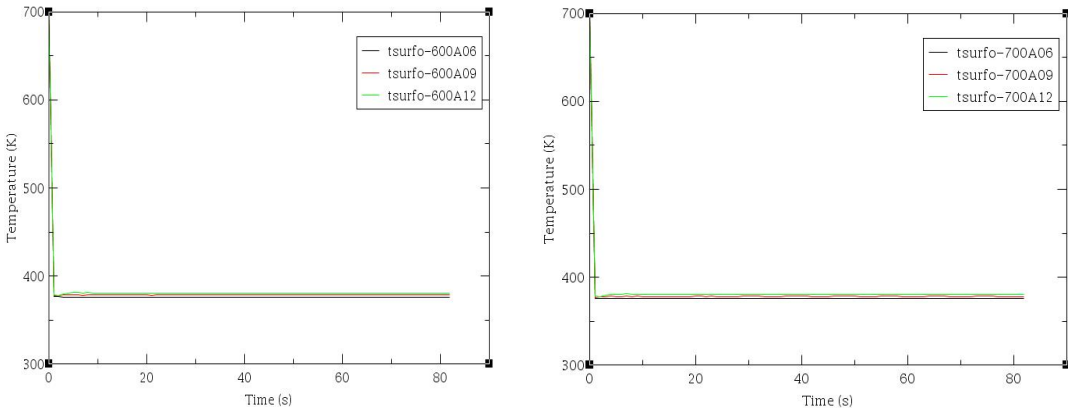

Figure 4.11: Mass flow rate in two channels and fuel outer surface temperature on steady state condition for case 3.

4.2.3.2 Transient analysis

Heat structure 600: the same plot includes the outer surf rod temp at axial level 6, 9, 12. It shows that the outer surface rod temperature at level 6 and 9 does not reach the saturation temperature of the fluid, while it does at level 12. This is the hotter rod, the rod at higher power (300 kW). Again, the upper part of the rod is cooled earlier than the lower part.

Heat structure 700: the same plot includes the outer surf rod temp at axial level 6, 9, 12. The point is that these temperatures decrease to the saturation temperature of the fluid. This is the rod at lower power (290 kW). Again, the upper part of the rod is cooled earlier than the lower part.

On the figure 4.12, the mass flow rate at axial level 6 in the pipes 400 and 500 are showed. Pipe 500 has a higher mass flow rate, so the associated rod (heat structure 700) is better cooled.

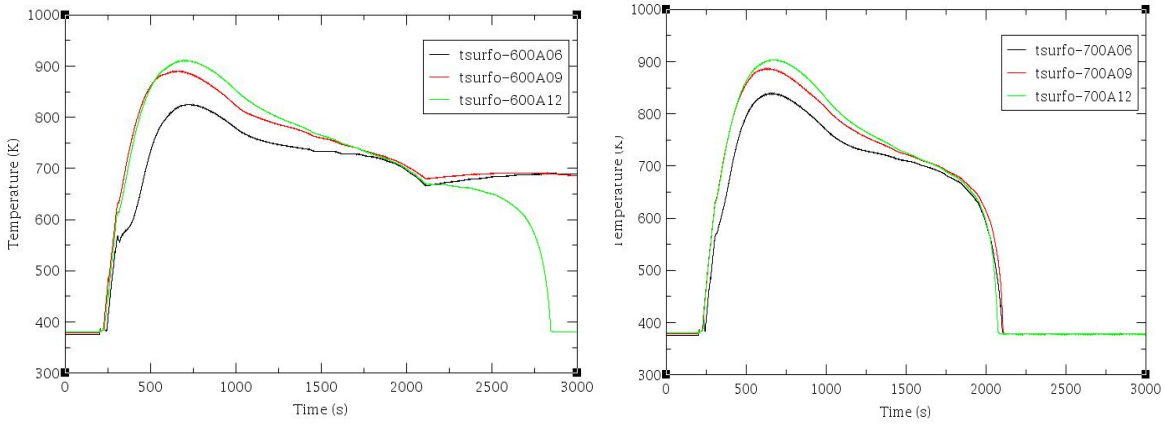

Figure 4.12: Mass flow rate in two channels and fuel outer surface temperature on transient state condition for case 3.

4.2.4 Comparison among the 3 cases

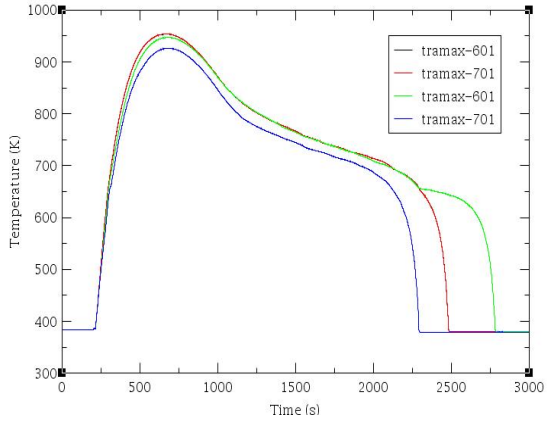

Figure 4.13: The comparison between the max average temperature by power component 601 and power component 701 for the cases 1 (300-300 kW) and 2 (300-295 kW).

In figure 4.13, legend tramax refers to maximum average temperature of a particular fuel assembly. Black and red curves indicate the maximum average temperature for case 1 and green and blue curves indicate the maximum average temperature for case 2. The black curve is not visible since the delivered power for two distinct fuel assemblies are same.

In case 1 and case 2, the surface rod temperature is approximately reduced to the saturation temperature of the coolant; in case 2, this reduction occurs later for the hotter channel.

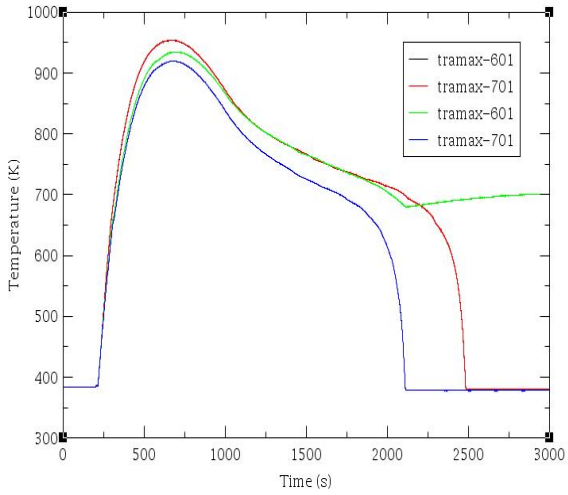

Figure 4.14: The comparison between the max average temperature by power component 601 and component 701 for the cases 1 (300-300) and 3 (300-290).

In figure 4.14, black and red curve indicate the max average temperature of two fuel assemblies for case 1 and green and blue curve indicate the max average temperature for case 3. The black curve is not visible since the delivered power for two distinct fuel assemblies for case 1 are same.

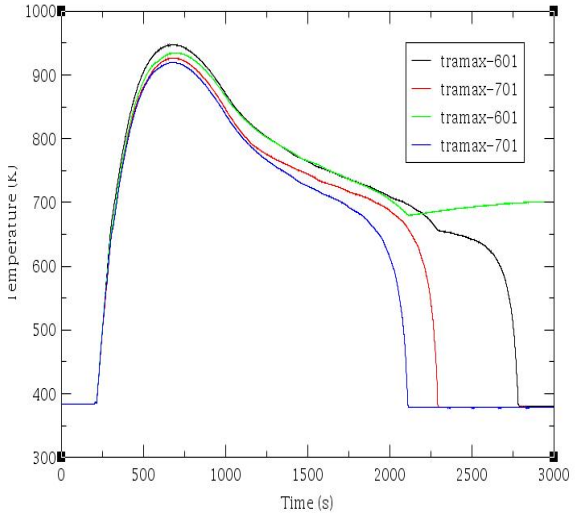

Figure 4.15: The comparison between the max average tempareture by power component 601 and component 701 for the cases 2 (300-295) and 3 (300-290).

In figure 4.15, black and red curve indicate the max average temperature of two fuel assemblies for case 2 and green and blue curve indicate the maximum average temperature of two fuel assemblies for case 3.

In case 2, the surface rod temperature is approximately reduced to the saturation temperature of the coolant within the calculation time of 3000 seconds; in case 3, it does not occur for the hotter channel and the mass flow rate is smaller.

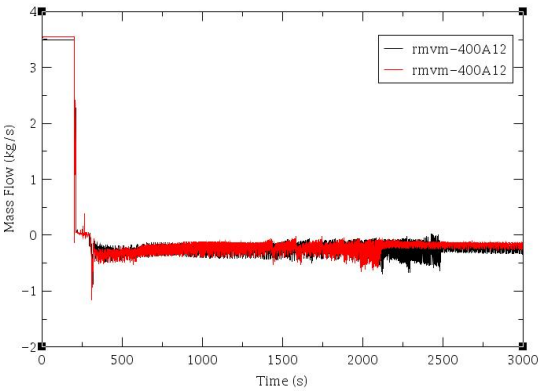

Figure 4.16: The comparison between the mass flow rate of pipe 400, at axial level 12, for the cases 1 (300-300) and 3 (300-290).

In figure 4.16, legend rmvm refers to mass flow rate along a particular channel .400 and 12 respectively refers to the component number and level number of the component. Black and red curves consecutively indicate the mass flow rate for case 1 and case 3.

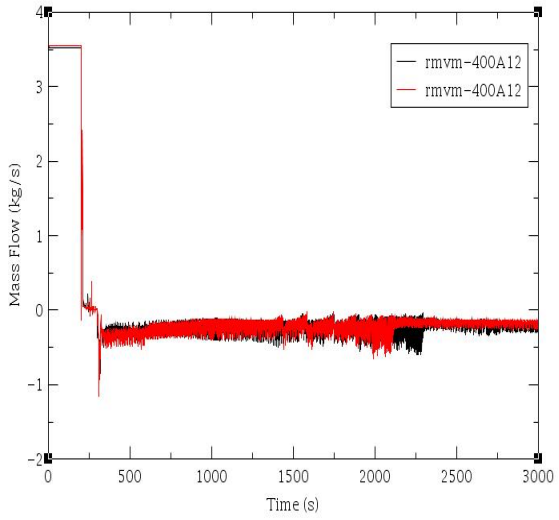

Figure 4.17: The comparison between the mass flow rate of pipe 400, at axial level 12, for the cases 2 (300-295) and 3 (300-290).

In figure 4.17, black and red curve consecutively indicate the mass flow rate for case 2 and case 3.

The point is that power differences between the two heated channels lead to differences in the mass flow rates to the channels. This, in turn, affects the reflooding process. In comparison with two above figures, more power causes more boiling and counters current flow .As a result, higher range of magnitude is found for case 1, in comparison with case 2 and case 3. Most importantly, the mass flow rate along the channel is negative since flow direction in transient state is opposite to the steady state.

For instance, it is seen that the maximum average temp in the hotter channel of case 2 is reduced to the saturation temperature of the fluid, while it does not happen in case 3 for the hotter channel during the calculation time of 3000 seconds. In fact, even though the total power of case 2 is higher the more even power distribution between the two channels seems to give better conditions for the decrease of temperature in the hotter channel. In fact, the mass flow rate of pipe 400 in case 2 is higher than the mass flow rate of pipe 400 in case 3.

Chapter 5

Summary and conclusions

A simplified TRACE model was developed for two parallel BWR fuel assemblies with an emergency cooling system injecting water from the top. This is applied to investigate possible effects of different power levels in the two channels, on the evolution of the reflooding phase that follows a loss of coolant. Three cases were analyzed. According to these calculations, it was shown that in cases 1 and 2, where the initial power provided to the two channels is more evenly distributed, the maximum average rod temperature of the hotter channel is quenched and decreases to the saturation temperature of the fluid within the simulation time of 3000 seconds. On the other hand, in case 3, where the difference between the power of the two rod bundles is larger (the initial power in the two channels is equal to 300 and 290 kW, respectively), the temperature of the hotter channel cannot be reduced to the coolant saturation level as quickly as the other cases.

It must be emphasized that the model has several limitations (as explained in chapter 3). In addition to this, more TRACE code options should be implemented such as fine mesh reflood and axial heat conduction, a radiation model could be added up to obtain more accurate results .Moreover, all rods of the fuel assembly could be divided into several groups to obtain more accurate result. Better assumptions of other parameters (boundary condition) lead to better evaluation of the quenching of the heated surface and thus exact result of the outer heated surface is achievable. In comparison with previous study of Gota facility experiment, this simulation is performed for two parallel heated channels instead a single channel and the variation in the mass flow and the outer surface temperature of fuel rods along the two parallel channels with respect to the change in delivered power are mainly discussed in this work.

Future work would be needed in order to address them and thus predict a more realistic behavior of the system.

.

6 References

[1]Nuclear Energy agency.(2007) What role for nuclear energy? [Online]

http://www.oecd-nea.org/press/2007/echavarri-g8.html

[2]AREVA. (2013) Nuclear Reactor technologies. [Online]

http://www.areva.com/EN/operations-1618/nuclear-reaction-one-principle-and-three-reactors-technologies.html

[3] Nordlund, Anders. "Introduction to nuclear reactors." ***Chalmers Tekniska Högskola*** **(2012).**

[4] World Nuclear Association.(2014) Nuclear Power reactors.[Online]

http://www.world-nuclear.org/info/nuclear-fuel-cycle/power-reactors/nuclear-power-reactors/

[5] David A. McMurrey. Online technical writing developing reports-Note taking.[Online]

https://www.prismnet.com/~tcm/images/TWNOTE2.GIF.

[6]SMF 2.0.8(2014).Prison planet Forum.[Online]

http://nuclearstreet.com/images/img/abwrcutaway.jpg

Nuclear Fuel Industries, Ltd.(2006).Light-Water Reactor Fuel.[Online]

http://www.nfi.co.jp/e/product/images/prod02_BWR.jpg

[7] Bajorek, S. "TRACE V5. 0 Theory Manual, Field Equations, Solution Methods and Physical Models." ***United States Nuclear Regulatory Commission*** **(2008).**

[8] TRACE V5.0 USER'S MANUAL Volume 2 : Modelling Guidelines by United States Nuclear Regulatory Commission .

[9] Applied Programming Technology, Inc. (2007-2011) Aptplot overview.[online]

https://www.nrcsnap.com/aptplot/overview.jsp.

[10]TRACE V5.0 USER'S MANUAL Volume 1 : input specification by United States Nuclear Regulatory Commission.

[11] Racca, Stefano, and Tomasz Kozlowski. "Trace code validation for BWR spray cooling injection and CCFL condition based on GÖTA facility experiments."*Science and Technology of Nuclear Installations* 2012 (2011).